Two Univalent Electron Transfers from Putidaredoxin to Bacterial Cytochrome P_{450} at Subzero Temperature†

Gaston Hui Bon Hoa, Evelyne Begard, Pascale Debey,* and I. C. Gunsalus‡

ABSTRACT: A full dynamic description of the multistep multienzyme O_2 reduction and hydroxylation sequence remains a challenge worthy of multiple approaches. Experimentation in fluid media at subzero temperatures allows one to exploit the differences in activation energy and to resolve the overall process into the two univalent reductions of the cytochrome P_{450} by the natural electron donor, putidaredoxin. We consider first the initial ferric/ferrous reduction of a P_{450} cytochrome–substrate complex. The kinetics are analyzed after rapid mixing of chemically reduced putidaredoxin with the P_{450} over the temperature range −10 to −40 °C. With increases in the initial putidaredoxin level, the ferrous P_{450} yield reaches an apparent plateau near 60% reduction. Analysis of the kinetics indicates the primary, and rate-limiting, event is the formation of a dienzyme complex followed by a reversible intermolecular electron transfer. The reduction rate depends directly on the putidaredoxin concentration in the 1 to 25 μM range; the activation energy of the rate constant is 11 kcal/mol. The second single-electron transfer, to the cytochrome P_{450}, and product formation are conveniently studied at subzero temperature, since the oxy-ferrous complexes, both with and without camphor, are stable for hours below −20 °C in a fluid hydroorganic medium, and can thus be used as starting reagents. The process is studied in two steps: (1) the reaction cycle, initiated by the full reduction of both cytochrome and putidaredoxin at +10 °C, gives the equilibrium Fe^{2+}·RH + $Pd^{-} \rightleftharpoons Pd^{-}$–$Fe^{2+}$·RH; (2) oxygen addition at −10 to −40 °C "activates" the system, while side pathways of spontaneous decay and recycling, e.g., rebinding of substrates, are effectively "quenched". The multistep enzyme catalysis FeO_2^{2+}·RH + $Pd^{-} \rightarrow Fe^{3+}$ + Pd^{O} + ROH + H_2O is rate limited by the first-order decomposition of an intermediate, and the activation energy is 11.5 kcal/mol.

Dioxygen reduction in heme P_{450} coupled monoxygenases via an ordered cyclical sequence of alternate substrate addition and univalent reduction has been well documented (Estabrook et al., 1968; Gunsalus et al., 1971, 1974; Peterson et al., 1973). The importance of a model system to elucidate the kinetic and thermodynamic parameters that regulate the P_{450} monoxygenase process is emphasized by the multiplicity, ubiquity, and similarities in the catalytic centers implied by optical and other resonance spectra in the reaction sequences and protein size.

The liquid mixed solvent subzero temperature method of Douzou (1975, 1977) offers several theoretical advantages for the possible temporal resolution of reactions into elementary steps according to activation energies (Douzou et al., 1970), stabilization of labile intermediates, and discrimination of individual pathways within a set of alternative reaction processes (Douzou, 1973).

The various redox states of the bacterial P_{450} cytochrome and of putidaredoxin have been investigated by systematic low-temperature studies in fluid solvents at normal and subzero temperatures. The hydroorganic solvent mixtures employed have been shown to induce only discrete and *reversible* perturbations of conformation equilibria within each state which do not differ from those induced by mere "physiological" parameters (Lange et al., 1977a). Aside from these solvent effects, the cytochrome is not denatured, nor is the basic reaction sequence altered. Meanwhile, the less stable oxy-ferrous complex, the real starting species for the hydroxylation, is stabilized and used as pure reagent (Eisenstein et al., 1977; Debey et al., 1976). The true hydroxylation step(s) could be studied only after overcoming the critical difficulties, especially, rapidity of the reaction, instability of the ternary oxygenated compound (FeO_2^{2+}·RH), and recycling of the free ferric enzyme (Fe^{3+}) by the camphor and putidaredoxin components necessarily present in excess.

The main thrust of this paper is to present a low-temperature spectroscopic study of the mechanism of the *first* and *second* electron transfers from putidaredoxin to, respectively, Fe^{3+}·RH and FeO_2^{2+}·RH. This systematic kinetic and thermodynamic analysis over the subzero temperature range of −10 to −40 °C is both possible and fruitful because the reaction rates are drastically slowed down at these temperatures.

Materials and Methods

The bacterial cytochrome P_{450} and putidaredoxin were prepared in the laboratory by one of us (I.C.G.) by an automated modification of the procedure of Yu et al. (1974); see Gunsalus and Wagner (1978). The reagents were acquired from standard sources and used without further purification; the D-camphor and acridine orange are Merck products, pure ethylene glycol (EGOH[1]) is from Carlo Erba, and EDTA is from Calbiochem.

† From the Service de Biospectroscopie, Institut de Biologie Physico-Chimique, 75005 Paris, France. *Received October 15, 1976; revised manuscript received March 2, 1978.* Supported in part by grants from DGRST (Contract No. 71.7.3091), CNRS (Equipe Associée No. 262), DRME (Contract No. 73/473), Fondation pour la Recherche Médicale Francaise (P.D. and E.B.), and the United States National Institutes of Health, Institute of Arthritis, Metabolism, and Digestive Diseases (HEW PHS AM 00562) (I.C.G.).

‡ Present address: Biochemistry Department, University of Illinois, Urbana, Illinois 61801.

[1] Abbreviations used: EGOH, ethylene glycol; EDTA, ethylenediaminetetraacetic acid (disodium salt); Fe^{3+}·RH, Fe^{2+}·RH, and FeO_2^{2+}·RH, cytochrome P_{450} substrate bound, reduced substrate bound, and reduced substrate bound oxygenated, respectively; Pd^{O} and Pd^{-}, oxidized and reduced putidaredoxin.

0006-2960/78/0417-2835$01.00/0

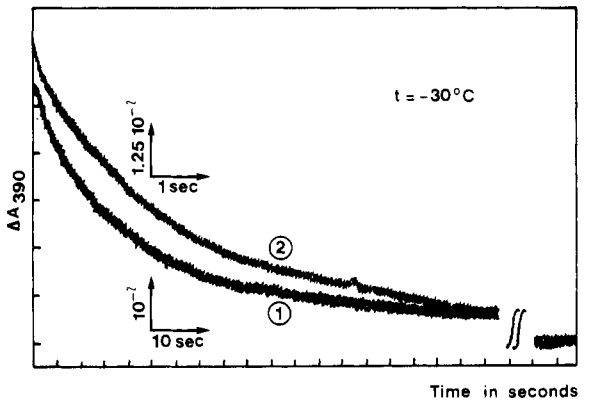

FIGURE 1: Kinetics of Fe^{3+}·RH reduction by Pd^{-}. Stopped-flow at subzero temperatures. Solvent: 1:1 (v/v) 100 mM phosphate buffer (pH 7) and EGOH, containing 200 mM KCl and 3 mM camphor as final concentrations; monitoring wavelength 390 nm; e_0 = 4.6 μM Fe^{3+}·RH; s_0 = Pd^{-}; t = −30 °C; one, s_0 = 3.8 μM; two, s_0 = 25.3 μM.

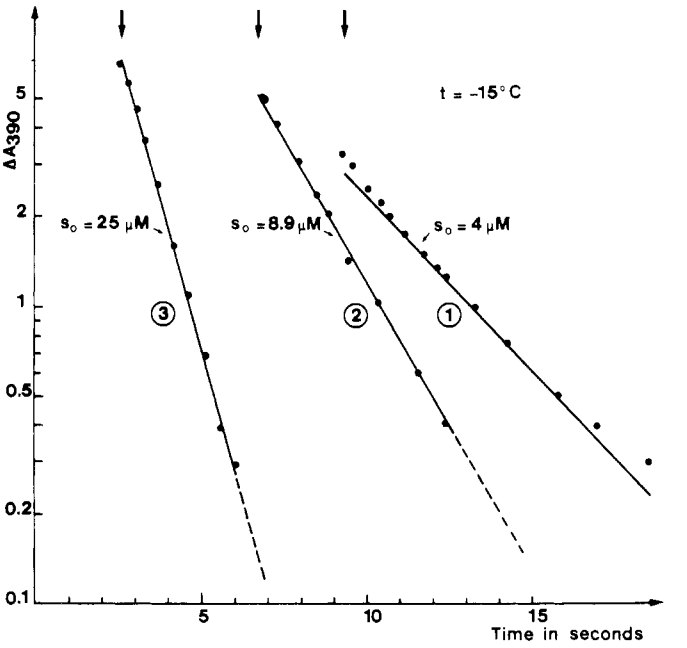

FIGURE 2: Semilogarithmic plots of the kinetics of Fe^{3+}·RH reduction by Pd^{-}. Solvent as in Figure 1: $-t$ = −15 °C; e_0 = 4.6 μM; one, s_0 = 4 μM; two, s_0 = 8.9 μM; three, s_0 = 25 μM. The arrows indicate time t = 0.

The solvent is 1:1 (v/v) 0.1 M potassium phosphate buffer (pH 7) and ethylene glycol (EGOH); at 20 °C, the "paH" is approximately 0.5 unit above the pH of the starting aqueous buffer and it increases only slightly as the temperature is decreased to the freezing point (Hui Bon Hoa and Douzou, 1973a; Douzou, 1977). The concentrations of KCl and camphor, which are critical, are specified in each case.

The cytochrome P_{450} and putidaredoxin are dissolved directly in the mixed solvent at +4 °C and checked for denaturation (especially transformation of cytochrome P_{450} into cytochrome P_{420}). Solvent effects on protein conformation, for example, perturbation of the cytochrome spin-state equilibrium, are fully reversible by dilution in water and do not differ from those induced by more physiological parameters (Lange et al., 1977a). Enzyme stock solutions were stored in the fluid mixed solvent at −20 to −30 °C, to avoid repetitive freezing-thawing cycles. Putidaredoxin at 10 μM retains 80% of full activity during 2 months storage at −20 °C in the 1:1 phosphate buffer-EGOH mixture, whereas rapid destruction occurs in 24 h at +4 °C, or after successive freezing-thaw cycles.

Reduction is induced either by a limited amount of sodium dithionite (~10^{-5} M) or by light. The photochemical reduction is accomplished by supplementing the protein solution with 1.9 to 2.5 μM acridine orange and ~1 mM EDTA and deoxygenating by bubbling for 30 min in an anaerobic cell with pure nitrogen or argon and then irradiating for several minutes at +10 °C with a 450-W xenon lamp set perpendicular to the sample cuvette of an Aminco Chance D W2 spectrophotometer (Greenbaum et al., 1972). UV and heat filters are introduced in the light beam.

Spectra and kinetics are recorded with an Aminco-Chance DW 2 spectrophotometer equipped for thermal control between +40 and −80 °C (Maurel et al., 1974) or with a stopped-flow specially designed for rapid mixing (dead time less than 3 ms) even at very low temperature (−40 °C) (Hui Bon Hoa and Douzou, 1973b).

Results and Discussion

Reduction of Ferric Substrate Cytochrome. Figure 1 is a kinetic trace of cytochrome P_{450} reduction by reduced putidaredoxin at −30 °C after stopped-flow mixing. The Pd^{O} reduced previously to Pd^{-} at 20 °C by limited amounts of dithionite (10^{-5} M) had been stored at −25 °C in a closed syringe. The rate of direct reduction of Pd^{O} or of Fe^{3+}·RH by dithionite at subzero temperatures is too slow to be taken into account, and the eventual formation of FeO_2^{2+}·RH is avoided by complete deoxygenation of the Fe^{3+}·RH solution.

At high Pd^{-} concentrations, s_0 = 10–25 μM, cytochrome reduction follows first-order kinetics, as shown by the linear plots of log ΔA vs. t in Figure 2. The line slopes depend linearly on $[s_0]$, the initial Pd^{-} concentration, up to at least 25 μM. The second-order rate constants are, respectively, at −10 and −40 °C, 5 × 10^4 and 6 × 10^3 M^{-1} s^{-1}; the activation energy E_a is 11 ± 1 kcal/mol.

When the final concentration of reduced cytochrome (x_e) is plotted as a function of the initial Pd concentration (s_0) (Figure 3), a smooth saturation curve with a plateau at 60% reduction is found at −14 and −28 °C, as shown respectively by curves 1 and 2. Thus, the whole process is composed only of reversible steps. The simplest scheme that could represent the process would be a reversible bimolecular reaction:

$$Fe^{3+}\cdot RH + Pd^{-} \underset{l}{\overset{k}{\rightleftharpoons}} Fe^{2+}\cdot RH + Pd^{O}$$

yielding to

$$x_e^2 = k(s_0 - x_e)(e_0 - x_e)/l \qquad (1)$$

where e_0 is the initial cytochrome concentration. For high values of s_0, x_e should tend toward e_0; the variation of x_e for k/l approaching unity is plotted as curve 3 of Figure 3. Comparison of curve 3 with the experimental curves clearly shows that this scheme cannot describe properly the reduction process.

The "apparent" plateau at 60% reduction implies a more complex pathway, for example, a binding of the two proteins before electron transfer, tentatively schematized as follows:

$$Fe^{3+}\cdot RH + Pd^{-} \underset{k_{-1}}{\overset{k_1}{\rightleftharpoons}} Pd^{-}\text{-}Fe^{3+}\cdot RH \underset{l}{\overset{k}{\rightleftharpoons}}$$

$$(X_1)$$

$$Pd^{O}\text{-}Fe^{2+}\cdot RH \underset{k_2}{\overset{k_{-2}}{\rightleftharpoons}} Pd^{O} + Fe^{2+}\cdot RH \qquad (2)$$

$$(X_2)$$

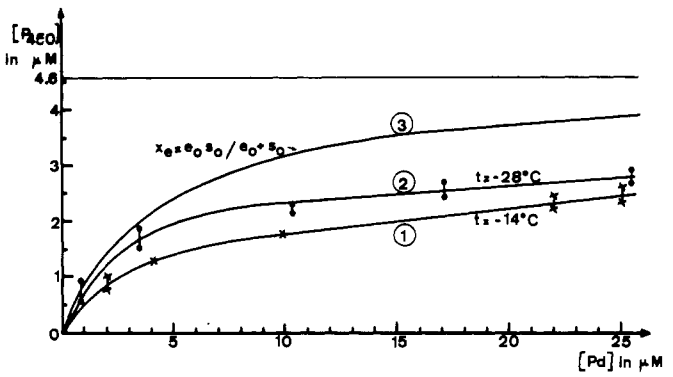

FIGURE 3: Final concentration of Fe^{2+}·RH (x_e) as a function of initial concentration of Pd^- (s_0). Solvent as in Figure 1: one, $t = -14$ °C; two, $t = -27$ °C; three, calculated curve for a reversible bimolecular reduction (eq 1; see text).

In such a scheme the reduction yield would be limited mostly by the forward and reverse electron transfers within a single complex of constant composition. This conclusion agrees with the results of Gunsalus and Sligar (1976), who demonstrated by various techniques the formation of putidaredoxin and cytochrome P_{450} dienzyme complexes in aqueous buffer, at least when both proteins are either oxidized or reduced. A substantial increase was found in the redox potential of Pd upon binding with Fe^{3+}·RH (from −240 to −196 mV), which reduces the free energy of electron transfer and favors the reversibility (Sligar, 1976; Sligar and Gunsalus, 1976).

This scheme to be complete must include the eventual binding of Pd^- to Fe^{2+}·RH and Pd^O to Fe^{3+}·RH, yielding the following "abortive" complexes:

$$Pd^O + Fe^{3+}\cdot RH \underset{k_{-3}}{\overset{k_3}{\rightleftharpoons}} Pd^O\text{-}Fe^{3+}\cdot RH \qquad (X_3) \quad (3)$$

$$Pd^- + Fe^{2+}\cdot RH \underset{k_{-4}}{\overset{k_4}{\rightleftharpoons}} Pd^-\text{-}Fe^{2+}\cdot RH \qquad (X_4) \quad (4)$$

Reaction 3 reduces the free Fe^{3+}·RH accessible to Pd^-; however, under the concentrations used—maximum Pd^O, free and complexed, is 2.6 μM, and minimum Fe^{3+}·RH is 2.6 μM—the contribution of equilibrium 3 should be rather low, since a K_d in the range of 40 μM has been found for the binding of Pd^O to Fe^{3+}·RH in hydroorganic medium at low temperature (Debey et al., 1977).

On the other hand, reaction 4 should drive the overall process toward more reduction by lowering the concentration of free Fe^{2+}·RH, to reach 100% reduction at saturating concentrations of Pd^-. We must assume that this equilibrium too has a negligible contribution to our conditions, since the increase in the reductive yield between 10 and 25 μM of Pd^- is very small (see Figure 3).

The redox transfer between the two species at relatively similar concentrations is a difficult problem to treat as a classical enzyme-catalyzed reaction. Thus, a study of the whole time course of the reaction, which is recordable, seems more appropriate. Several mechanistic hypotheses have been examined depending on the affinities of the proteins and the relative speeds of complex formation (k_1, k_{-1}, k_2, k_{-2}) and of electron transfer (k, l). Under our experimental conditions at low temperatures in hydroorganic solvents, simultaneous high affinity and fast binding of Pd^- to Fe^{3+}·RH must be ruled out, since this would lead to [Pd^-] independent first-order kinetics, controlled by the electron transfer from X_1 to X_2. Among the hypotheses we have considered, the best fit to the results is obtained by assuming that the binding of Pd^- to the

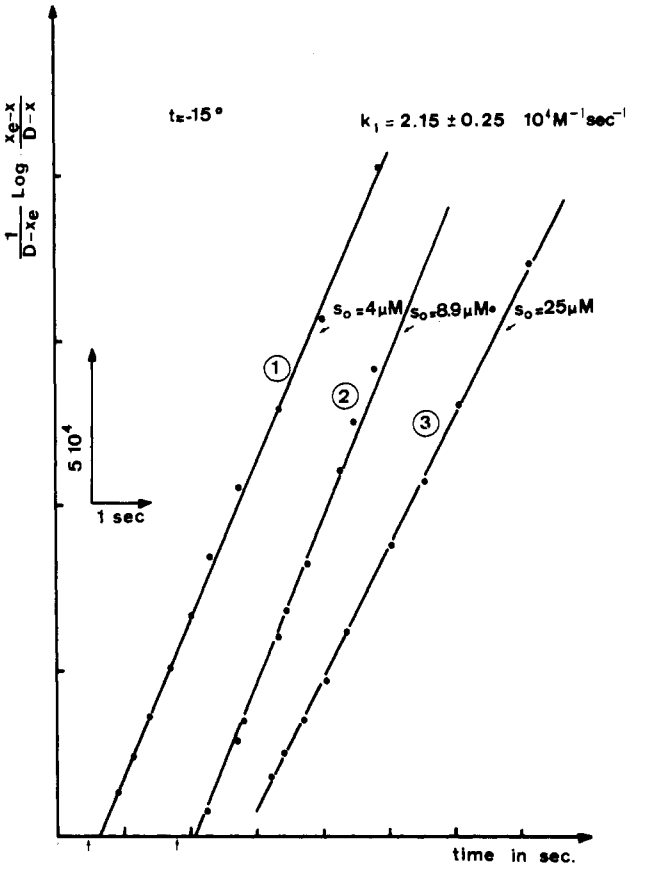

FIGURE 4: $(1/x_e - D) \log (x_e - x/D - x)$ as a function of time t according to eq 5: $\alpha = 1.4$; x_e measured from the total reduction yield; D calculated from the known values of x_e, s_0, e_0, as given in the text.

cytochrome molecule is rate limiting but tight, and is followed by a more rapid intermolecular electron transfer. In that case, one may assume an equilibrium between X_1 and X_2, since the electron equilibrates rapidly $kx_1 = lx_2$ where $x_1 = [X_1]$ and $x_2 = [X_2]$. Furthermore, if x is the concentration of the reduced cytochrome, either free or complexed, $x \simeq x_2$ if the association constant is high. Then

$$dx_1/dt + dx/dt = k_1(e_0 - x - x_1)(s_0 - x - x_1) - k_{-1}lx/k$$

$$\alpha dx/dt = k_1(e_0 - \alpha x) - k_{-1}lx/k$$

where $\alpha = 1 + l/k$. Finally,

$$\frac{1}{x_e - D} \log \left(\frac{e_0 s_0}{\alpha^2 x_e^2} \frac{x_e - x}{D - x} \right) = k_1 \alpha t \qquad (5)$$

where $D = e_0 s_0 / \alpha^2 x_e$. Thus, a plot of $(1/x_e - D) \log (x_e - x/D - x)$ as a function of time should be linear with a slope $m = k_1\alpha$ independent of the initial concentrations of putidaredoxin (s_0) and cytochrome (e_0).

As shown in Figure 4, plots of the experimental kinetics according to eq 5 fit the theory quite well. The choice of $l/k = 0.4$, the value previously determined by Sligar and Gunsalus (1976) in aqueous buffer at 25 °C, yields to $k_1 = 2.25 \pm 0.25 \times 10^4$ M^{-1} s^{-1} at −15 °C. Changing the l/k value from 0.01 to 0.9 does not affect the linearity of the plots and leads to only small variations of k_1, i.e., from $1.9 \pm 1 \times 10^4$ to $4.3 \pm 0.5 \times 10^4$ in M^{-1} s^{-1}. From experiments performed between −10 and −40 °C an activation energy of 11 ± 0.5 kcal/mol can be calculated, yielding to an extrapolated estimation of $k_1 = 3.5 \pm 0.5 \times 10^5$ M^{-1} s^{-1} at +25 °C.

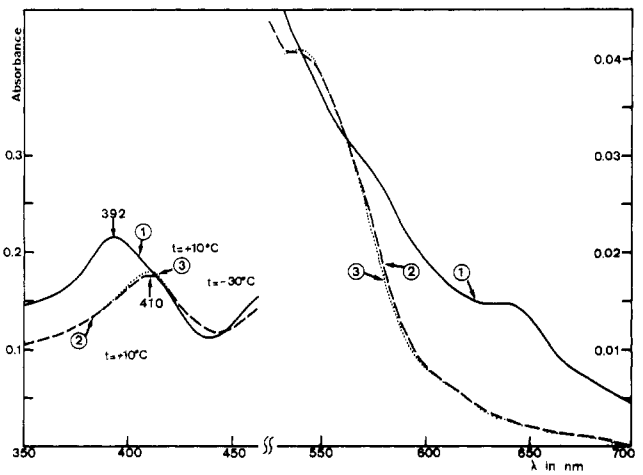

FIGURE 5: Absorption spectra of Fe^{3+}·RH + Pd^{O} mixture before and after reduction at several temperatures: one, oxidized cytochrome (2.1 μM) and putidaredoxin (7 μM) with 30 μM camphor, 200 μM KCl, 1 mM EDTA, and 2 μM acridine orange in 1:1 (v/v) 100 mM potassium phosphate buffer (pH 7)–EGOH (paH 7.4 at 20 °C) at +10 °C; two, following complete photochemical reduction at +10 °C; three, temperature decreased to −30 °C.

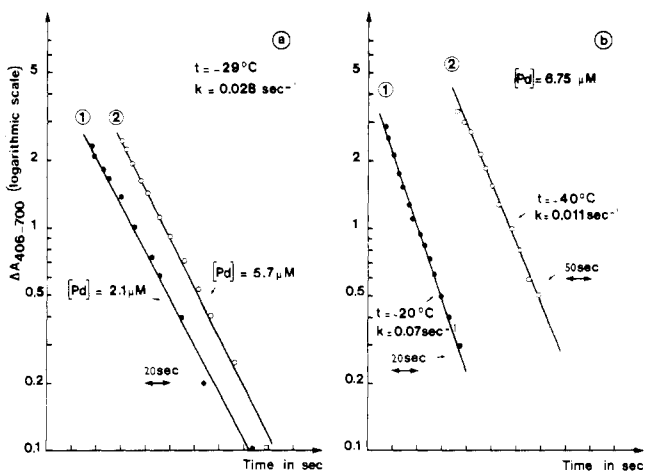

FIGURE 6: Decomposition rates of FeO_2^{2+}·RH by Pd^{-}. Solvent as in Figure 5, photochemical reduction followed by bubbling of oxygen (10 s). Optical absorption increase followed at 406 nm: (a) Effect of Pd^{-} concentration at −29 °C. Cytochrome concentration was 1.8 μM: Pd^{-} = one, 2.1 μM; two, 5.7 μM. (b) Effect of temperature. Cytochrome concentration was 2.1 μM; Pd^{-} concentration was 6.7 μM. The kinetics start, respectively, one, at −20 °C, 5 s, and, two, at −40 °C, 15 s after oxygen bubbling.

Furthermore, except for very low s_0 values, $D = e_0 s_0/\alpha^2 x_e \gg x$, so that $D - x \simeq D = e_0 s_0/\alpha^2 x_e$ and the simplified eq 5 becomes

$$\log\left(\frac{x_e - x}{x_e}\right) = -k_1\left(\frac{s_0 e_0}{\alpha x_e}\right) t \qquad (6)$$

in accordance with the linear semilogarithmic plots of log ($x_e - x$) vs. t obtained at high Pd^{-} concentration (Figure 2). Applying eq 6 to Figure 2 leads to $k_1 = 2.5 \pm 1 \times 10^4\ M^{-1}\ s^{-1}$, consistent with the above value.

The 25 °C extrapolated value is 10^3 times slower than the value ($3 \times 10^8\ M^{-1}\ s^{-1}$) obtained in aqueous medium by Pederson et al. (1977). This discrepancy could reflect a solvent effect on the association rate and affinity of the two proteins, which is now under close investigation. It does not change the model of the reduction occurring by intermolecular electron transfer within a functional bimolecular complex.

Reduction of Ferrous Oxycytochrome and Product Formation. The transfer of a second electron from Pd^{-} to FeO_2^{2+}·RH triggers a reaction sequence culminating in product, ROH, formation. A differential temperature effect was used to follow this process. A mixture of Fe^{3+}·RH and Pd^{O} is reduced photochemically at +15 °C in hydroorganic medium and the oxy intermediate is formed by bubbling with O_2 after cooling to a given subzero temperature. The reduction is accomplished as described under Materials and Methods; methylviologen is avoided because even at low temperature it causes a rapid reoxidation of Pd^{-} on bubbling of oxygen. The camphor concentration used, 20 to 30 μM, is five to ten times greater than the dissociation constant obtained by Lange et al. (1977b) from subzero temperature kinetic measurements under identical experimental conditions. After complete reduction of both components, as judged from the change in absorbance from the known cytochrome spectrum (Figure 5) relative to 404 nm, isosbestic between Fe^{3+}·RH and Fe^{2+}·RH, the cuvette is cooled under irradiation to a low temperature, e.g. −40 °C, and FeO_2^{2+}·RH is formed by a 5- to 10-s bubbling of oxygen.

The subsequent decomposition into Fe^{3+} is shown in Figure 6. The rates are monophasic, first order, with half-times dependent only on the temperature and independent of the initial Pd^{-} concentration. The respective $t_{1/2}$ values at $t = -20$ and −40 °C are 9.9 and 63 s, and the activation energy, from experiments performed between −10 and −40 °C, is calculated to be 11.5 ± 0.5 kcal/mol.

The product yield on decomposition is not stoichiometrically related to the cytochrome or putidaredoxin concentrations but follows a saturation curve with a plateau at 100% transformation and an affinity constant of approximately 1.5 μM for the electron-donating species.

By analogy of this second electron-transfer process with the first reduction, the following minimal sequence of events can be proposed for the decomposition of the oxyferro cytochrome by reduced putidaredoxin:

$$Pd^{-} + FeO_2^{2+}\cdot RH \rightleftharpoons Pd^{-}\text{–}FeO_2^{2+}\cdot RH \rightleftharpoons (X_1') \rightarrow Pd^{O} + Fe^{3+} + ROH$$

However, in this instance, the problem can be simplified by starting the reaction from the X_1' complex. In the absence of putidaredoxin, the ferrous oxycytochrome P_{450}, FeO_2^{2+}·RH, is stable for hours at subzero temperatures (Eisenstein et al., 1977).

Furthermore, in cosolvent at subzero temperatures and camphor at 30 μM the half-time of its binding and the reduction rate by the first electron are much slower than the decomposition process (Lange et al., 1977b). Thus, by starting with the preformed dienzyme complex, Pd^{-}–Fe^{3+}·RH, the decomposition of the oxygenated complex at low temperatures is "uncoupled" from the subsequent recycling ($Fe^{3+} \rightarrow Fe^{3+}$·RH → Fe^{2+}·RH → FeO_2^{2+}·RH) and from spontaneous nonhydroxylating decay (FeO_2^{2+}·RH → Fe^{3+}·RH + O_2 + e^{-}). This allows a clear view of the reaction not possible at room temperature. Interference from camphor rebinding is further avoided by monitoring at 406 nm, a wavelength isosbestic between Fe^{3+} and Fe^{3+}·RH. Thus, the kinetics recorded represent only the enzymatic decomposition of the active ferrous-oxysubstrate-heme complex catalyzed by the reduced putidaredoxin. The monophasic, [Pd^{-}]-independent kinetics show clearly that the whole process is rate limited by the decomposition of an intermediate compound, the nature of which is still unknown. The affinity constant observed for the de-

composition reflects most probably the K_d of the binary Fe^{2+}-Pd^- complex.

More experiments are needed to reveal the more elementary process underlying oxygen activation and substrate hydroxylation. It is our feeling that faster kinetics combined with low temperatures could be very helpful in this respect.

Acknowledgments

The authors express their gratitude to Dr. P. Douzou for his constant interest in the work and stimulating advice and discussions.

References

Debey, P., Balny, C., & Douzou, P. (1976), *FEBS Lett. 69,* 231-235.

Debey, P., Hui Bon Hoa, G., & Gunsalus, I. C. (1977), *Croat. Chem. Acta 49,* 309-321.

Douzou, P. (1973), *Mol. Cell. Biochem. 1,* 15-27.

Douzou, P. (1975), *Methods Biochem. Anal. 22,* 401-512.

Douzou, P. (1977), Cryobiochemistry, An Introduction, London, Academic Press.

Douzou, P., Sireix, R., & Travers, F. (1970), *Proc. Natl. Acad. Sci. U.S.A. 66,* 787-792.

Eisenstein, L., Debey, P., & Douzou, P. (1977), *Biochem. Biophys. Res. Commun. 77,* 1377-1383.

Estabrook, R. W., Hildebrandt, A., Remmer, H., Schenkman, J. B., Rosenthal., O., & Cooper, D. Y. (1968), *Colloq. Ges. Biol. Chem. 19,* 142.

Estabrook, R. W., Schenkman, J. B., Cammer, W., Remmer, H., Cooper, D. Y., Narashimhulu, S., & Rosenthal, O. (1966), in Biological and Chemical Aspects of Oxygenases, Bloch, K., & Hayaishi, O., Ed., Tokyo, Maruzen Co., p 153.

Greenbaum, E., Austin, R. H., Frauenfelder, H., & Gunsalus, I. C. (1972), *Proc. Natl. Acad. Sci. U.S.A. 69,* 1273-1276.

Gunsalus, I. C., Meeks, J. R., Lipscomb, J. D., Debrunner, P., & Münck, E. (1974), in Molecular Mechanism of Oxygen Activation, Hayaishi, O., Ed., New York, N.Y., Academic Press, pp 559-613.

Gunsalus, I. C., & Sligar, S. G. (1976), *Biochimie 58,* 143-147.

Gunsalus, I. C., Tyson, C. A., Tsai, R. L., & Lipscomb, J. D. (1971), *Chem. Biol. Interact. 4,* 75-78.

Gunsalus, I. C., & Wagner, G. C. (1978), *Methods Enzymol. 51,* 166-188.

Hui Bon Hoa, G., & Douzou, P. (1973a), *J. Biol. Chem. 248,* 4649-4654.

Hui Bon Hoa, G., & Douzou, P. (1973b), *Anal. Biochem. 51,* 127-136.

Lange, R., Bonfils, C., & Debey, P. (1977a), *Eur. J. Biochem. 79,* 623-628.

Lange, R., Hui Bon Hoa, G., Debey, P., & Gunsalus, I. C. (1977b), *Eur. J. Biochem. 77,* 479-485.

Maurel, P., Travers, F., & Douzou, P. (1974), *Anal. Biochem. 57,* 555-563.

Pederson, T. C., Austin, R. H., & Gunsalus, I. C. (1977), in Proceedings of the Third International Symposium on Microsomes and Drug Oxidations, New York, N.Y., Pergamon Press, pp 275-283.

Peterson, J. A., Ishimura, Y., Baron, J., & Estabrook, R. W. (1973), in Oxidases and Related Redox Systems, King, T. E., Mason, H. S., & Morrison, M., Ed., Baltimore, Md., University Park Press, pp 565-577.

Sligar, S. (1976), *Biochemistry 15,* 5399-5406.

Sligar, S., & Gunsalus, I. C. (1976), *Proc. Natl. Acad. Sci. U.S.A. 73,* 1078-1082.

Yu, C.-A., Gunsalus, I. C., Katagiri, M., Suhara, K., & Takemori, S. (1974), *J. Biol. Chem. 249,* 94-101.